Journal of Sound and Vibration (2001) **247**(3), 453–469
doi:10.1006/jsvi.2001.3755, available online at http://www.idealibrary.com on IDEAL®

A MULTIPLE-INPUT MULTIPLE-OUTPUT SMOOTHING TECHNIQUE: THEORY AND APPLICATION TO AIRCRAFT DATA

R. RUOTOLO

Department of Aeronautical and Space Engineering, Politecnico di Torino, corso Duca degli Abruzzi 24, *Torino* 10129, *Italy. E-mail*: *ruotolo@athena.polito.it*

(*Received* 11 *September* 2000, *and in final form* 20 *March* 2001)

The aim of the research described in this article is to propose a technique for curve-fitting a modal model to frequency response functions (FRFs) in order to deal with multi-input multi-output (MIMO) systems with highly coupled modes, usually encountered in vibration testing. This new formulation permits a global model for the structure under test to be determined by estimating directly at the first step both poles and participation factors. Results related to numerical simulations and to the analysis of experimental data measured on an aircraft before performing a flight-flutter test complete the article.

1. INTRODUCTION

In the field of structural dynamics widespread use is made of modal testing, an experimental technique for evaluating the modal properties based on the assumption that the dynamic behaviour of the structure under test is nominally linear: it is common practice in various fields of engineering and is performed on complex structures such as spacecraft, aircraft, cars, trains, large machinery, etc. Moreover, as a result of extensive research performed in the field of system identification, a number of techniques can be applied to analyze the measured frequency response functions (FRFs) that are processed in order to obtain a reduced order mathematical modal model representing the dynamic characteristics of the structure over the finite bandwidth of the test data [1].

Although several alternatives for curve fitting measured FRFs are often available, the analyst applying such techniques regularly may need to overcome a series of practical difficulties, as highlighted by Van der Auweraer *et al.* [2], in order to obtain reliable results. In particular, each of the commonly available techniques, irrespective of whether the estimation process uses data in the time or frequency domain, suffers drawbacks when the structure exhibits a high degree of modal coupling, i.e., the presence of high damping and of close modes. In these cases very complex "stabilization diagrams" are obtained without giving any clear indication about the number and the position of the actual poles of the system under investigation.

It is well known that the analysis of data measured during flight-flutter test sessions is a challenging application for modal curve fitting since the measured signals are generally subject to high noise levels and the aircraft structure usually has high modal coupling [3]. Since, as extensively stated in section 3, the ultimate objective of this article is to develop a technique capable of curve fitting data measured on highly coupled systems, i.e., to address one of the problems listed in [2], in section 2 only those techniques are reviewed that have found application to problems of a relatively high level of complexity and usually requiring an iterative solution procedure, e.g., flight-flutter test data analysis.

2. REVIEW OF SOME CURVE-FITTING METHODS

Several alternatives for curve fitting measured FRFs are available, as described in references [1, 4–6]. In general, all the techniques permit curve fitting of the experimental data by minimizing a non-linear cost function that depends on the parameters present in the mathematical representation of the measured data [5]. Furthermore, in some methods the cost function is properly modified, so that it becomes a linear function of the parameters.

A first solution to the curve-fitting problem was given by Levi [7] who reduced the non-linear minimization problem to a linear least-squares problem by multiplying the cost function with the denominator of the FRF. This is a well-known technique but it suffers from overemphasis of high-frequency errors and provides biased estimates of the parameters to be estimated.

Sanathanan and Koerner [8] overcame the lack of sensitivity to low-frequency errors of the linear least-squares estimator proposed by Levi [7] by weighting the cost function and applying an iterative procedure. Many modifications and extensions to this technique have been published, as documented in reference [5].

Similar to the procedure adopted by Sanathanan and Koerner, the technique proposed by Dat and Meurzec [9] uses a cost function weighted by the denominator of the FRF; Lagrange multipliers permit the curve fitting to be formulated as an eigenvalue problem, the solution of which provides estimates for the natural frequencies and damping ratios of the structure under test. Originally, this method, called *Smoothing Technique*, was developed for single-input-single-output (SISO) systems and was successfully employed by the Italian aeronautical industry to analyze data acquired during flight-flutter test sessions, as documented in reference [10]. Provided that the procedure is convergent, the presence of the weighting function permits curve-fitting results of high quality to be obtained even if the system under test is highly damped and or with closed modes, as demonstrated in reference [11].

At the beginning of the 1970s it was common to estimate natural frequencies and damping ratios by performing a graphical analysis of the FRF. In order to circumvent the difficulties associated with graphical analysis (that provides erroneous values for the modal parameters for a number of reasons), Gaukroger *et al.* [12] proposed a technique based on an iterative linearized least-squares procedure to fit the receptance of a SISO system. The computer program derived by this algorithm was able to analyze frequency ranges with up to five modes and was designed in order to assist in the analysis rather than to automate the whole process.

The method developed by Goyder [13] permitted the modal parameters of each mode to be determined independently, so that the analyst gained more information during the estimation process, determining which mode is at fault if the procedure collapses; furthermore, this algorithm is able to analyze data measured at a number of response locations.

Pintelon *et al.* [14] proposed a parametric maximum-likelihood estimator to take into account the presence of noise on the input as well as on the output of the system under test, being capable of analyzing data measured on a SISO system and providing a solution to the estimation problem by minimizing a non-linear function. In reference [15], the authors extended this method so that it could deal with data measured at several stations and demonstrated its validity by analyzing flight-flutter data [16].

Having scope to analyze data measured during flight-flutter test sessions, an iterative frequency domain algorithm, called the instrumental variables output error method (IV/OEM), has been proposed by Emmett *et al.* [17] which does not require the minimization of a non-linear function [18]. As a result, it takes into account the total influence of errors due to measurement noise and the response to unmeasured aerodynamic excitations in order to provide the analyst with an assessment of the accuracy of each modal parameter identified. The method presented in reference [18] was a SISO technique, although the potential for extension to a multi-input multi-output (MIMO) version was suggested by the authors.

The capacity of a technique to analyze, in a single step, all the data measured by transducers placed at several locations of the system under test is very important for the practising engineer. When a SISO curve-fitting algorithm is applied to multiple-output measurements it is necessary to analyze every FRF separately, leading to a number of estimates for natural frequencies and damping ratios which would need to be averaged, for example, to obtain a single estimate.

To overcome this difficulty, during recent years the original procedure proposed in reference [9] has been extended, under the name of global smoothing technique (GST), in order to deal with multiple outputs in a single step. The related research activity is documented in references [19, 20], where it has been demonstrated that GST is capable of curve fitting FRFs measured during both flight-flutter tests and vibration tests on car suspensions, even if the topic of numerical conditioning of the procedure is not addressed in all its details.

This last problem has been considered in reference [11] and solved through the use of Forsythe's orthogonal polynomials [21], initially proposed for this kind of application by Van der Auweraer and Leuridan in their Orthogonal Polynomial method [22]. Moreover, in reference [11] FRFs measured on a fully trimmed car body have been analyzed, GST providing curve-fits of relatively high quality when compared with classical techniques based on the least-squares method.

3. AIM OF THIS ARTICLE

It is well known that multiple-input excitation is a convenient way of detecting closely spaced or double poles by the use of multiple-input modal-parameter estimation algorithms on multiple-input measurement data. As described in reference [1], since the mode shape coefficients are independent of the excitation location, multiple-input modal-parameter estimation methods will yield global estimates of these parameters.

The main drawback of the current formulation of GST is that it is capable of estimating only the poles of the system, while the estimation of the residue matrix of the partial fraction description [5] of the FRFs is performed by applying the least-squares frequency-domain method. Since the residue matrix is equal to the product of the mode shape matrix and the matrix of modal participation factors [23], when several inputs are present GST will provide as many estimates for a mode shape as the number of inputs.

As a consequence the aim of this article is to solve this estimation problem and make it possible for GST to provide a global modal model of the structure under investigation, in terms of mode shapes, poles and modal participation factors.

The determination of mode shapes and modal participation factors from the residue matrix has been addressed by various researchers, e.g., references [23, 24], and it may be a promising approach in the case of inconsistency in the data (in particular, non-reciprocal behaviour) as described in reference [2]. In these studies, this problem is solved by applying singular value decomposition in order to extract the best possible mode shapes, but in practical applications the residue matrix for each mode may have a rank greater than one, particularly when close modes are present, so that multiple modes are generated in the model even if they do not exist in the physical system, as underlined by Medina *et al.* [24].

As a consequence, the extension of the smoothing technique to the case of MIMO systems has been performed by following an approach similar to the orthogonal polynomial method [22], i.e., using a matrix fraction description for the FRF matrix. As shown in the following section, this extension maintains similar properties to those of the method proposed in reference [11], as well as retaining the behaviour of providing a high-quality curve fitting as demonstrated in section 5, where data measured on an aircraft before performing a flight-flutter test are analyzed.

4. FORMULATION OF THE MIMO SMOOTHING TECHNIQUE

4.1. BASIS OF THE METHOD

It is assumed that a set of $N_i \times N_o$ frequency response functions (where N_i is the number of inputs and N_o is the number of outputs present during the test) have been measured and collected into the [**H**] matrix. If the system under analysis is linear time invariant, according to reference [5] and [22], a matrix fraction description can be used to proceed with a frequency domain identification:

$$[\mathbf{H}(s)][\mathbf{A}(s)] = [\mathbf{B}(s)], \tag{1}$$

where $[\mathbf{A}(s)]$ is an $N_i \times N_i$ matrix, $[\mathbf{B}(s)]$ has dimensions $N_o \times N_i$ and $s = \mathrm{j}\omega$. Moreover, matrices $[\mathbf{A}(s)]$ and $[\mathbf{B}(s)]$ are polynomial functions of s with order n_a and n_b, respectively, i.e,

$$[\mathbf{A}(s)] = \sum_{r=0}^{n_a} [\mathbf{A}_r]s^r, \qquad [\mathbf{B}(s)] = \sum_{r=0}^{n_b} [\mathbf{B}_r]s^r, \tag{2}$$

where matrices $[\mathbf{A}_r]$ and $[\mathbf{B}_r]$ are real constants to be estimated in order to curve fit experimental data.

If [**H**] denotes the FRF matrix to be curve fitted, the error resulting from the approximation can be written as the difference between the right and the left side of equation (1), i.e.,

$$[\mathbf{e}(s)] = [\mathbf{H}][\mathbf{A}(s)] - [\mathbf{B}(s)] = \sum_{r=0}^{n_a} [\mathbf{H}][\mathbf{A}_r]s^r - \sum_{r=0}^{n_b} [\mathbf{B}_r]s^r \tag{3}$$

and by minimizing this error the method described in reference [22] can be derived.

In order to further extend the procedure originally proposed by Dat and Meurzec [9], it is possible to multiply both sides of equation (3) by $D(s)$, that is a weighting function to be selected following the criterium described subsequently:

$$[\mathbf{e}_w(s)] = \sum_{r=0}^{n_a} D(s)[\mathbf{H}][\mathbf{A}_r]s^r - \sum_{r=0}^{n_b} D(s)[\mathbf{B}_r]s^r. \tag{4}$$

The weighted unbalance of equation (1) is the error that must be minimized. Accordingly, it is possible to introduce a matrix of error functions given by

$$[\mathbf{J}(s)] = [\mathbf{e}_w(s)]^{\mathrm{H}}[\mathbf{e}_w(s)], \tag{5}$$

where the superscript H denotes complex conjugate transposition.

By introducing the matrix

$$[\mathbf{V}(s)] = D(s)[s^0[\mathbf{H}]s^1[\mathbf{H}], \ldots, s^{n_a}[\mathbf{H}] - s^0[\mathbf{I}] - s^1[\mathbf{I}], \ldots, - s^{n_b}[\mathbf{I}]] \tag{6}$$

and collecting all the unknown coefficients into the $[\mathbf{\Theta}]$ matrix

$$[\mathbf{\Theta}] = \begin{bmatrix} [\mathbf{A}_0] \\ \vdots \\ [\mathbf{A}_{n_a}] \\ [\mathbf{B}_0] \\ \vdots \\ [\mathbf{B}_{n_b}] \end{bmatrix} = \begin{bmatrix} [\mathscr{A}] \\ [\mathscr{B}] \end{bmatrix} \tag{7}$$

the matrix of error functions (5) can be rewritten as

$$[\mathbf{J}(s,[\mathbf{\Theta}])] = [\mathbf{\Theta}]^{\mathrm{T}}[\mathbf{V}(s)]^{\mathrm{H}}[\mathbf{V}(s)][\mathbf{\Theta}]. \tag{8}$$

4.2. MINIMIZATION OF THE ERROR MATRIX

To curve fit experimental data, it is necessary to minimize the fitting error over a given bandwidth I_ω, so that according to equations (4) and (5) it leads to the minimization of the following matrix depending on the coefficients $[\mathbf{\Theta}]$:

$$[\mathbf{J}([\mathbf{\Theta}])] = \int_{\mathrm{j}I_\omega} [\mathbf{J}(s,[\mathbf{\Theta}])]\,\mathrm{d}s = \Delta s \sum_{k \in I_k} [\mathbf{J}(s_k,[\mathbf{\Theta}])], \tag{9}$$

where it must be recalled that all FRFs have been measured at discrete values of the independent variable: $s_k = \mathrm{j}\omega_k$ with $k \in 1, \cdots, n_k = I_k$. Moreover, $\Delta s = s_{k+1} - s_k$ and matrix $[J([\mathbf{\Theta}])]$ has dimensions $N_i \times N_i$.

The minimization of the matrix of cost functions $[J([\mathbf{\Theta}])]$ is performed by considering a properly chosen norm of this matrix. It must be underlined that, in principle, any norm can be selected: in this study the trace of the matrix is chosen, i.e., the sum of terms along the principal diagonal $\sum_{i=1}^{N_i} J_{i,i}([\mathbf{\Theta}])$, mainly due to the convenience of this selection in the further reduction of the minimization process, as explained in the following.

According to expression (8) matrix $[\mathbf{J}]$ has non-negative values along the principal diagonal, so that the trace of the matrix can be minimized by minimizing, independently, every element $J_{i,i}(\{\mathbf{\Theta}_i\})$ on the diagonal of the matrix, where $\{\mathbf{\Theta}_i\}$ is the ith column of the coefficient matrix $[\mathbf{\Theta}]$.

Neglecting the factor Δs in equation (9), it can be reorganized as

$$[\mathbf{J}([\mathbf{\Theta}])] = [\mathbf{\Theta}]^{\mathrm{T}}[\mathbf{W}][\mathbf{\Theta}], \tag{10}$$

where matrix $[\mathbf{W}]$ has the structure

$$[\mathbf{W}] = \begin{bmatrix} [\mathbf{W}_{11}] & [\mathbf{W}_{12}] \\ [\mathbf{W}_{12}]^{\mathrm{H}} & [\mathbf{W}_{22}] \end{bmatrix} \tag{11}$$

with

$$[\mathbf{W}_{11}] = \sum_{k \in I_k} |D(s_k)|^2 \begin{bmatrix} q_{k,0}^*[\mathbf{Q}(s_k)]q_{k,0} & \cdots & q_{k,0}^*[\mathbf{Q}(s_k)]q_{k,n_a} \\ \vdots & \ddots & \vdots \\ q_{k,n_a}^*[\mathbf{Q}(s_k)]q_{k,0} & \cdots & q_{k,n_a}^*[\mathbf{Q}(s_k)]q_{k,n_a} \end{bmatrix},$$

$$[\mathbf{W}_{12}] = \sum_{k \in I_k} |D(s_k)|^2 \begin{bmatrix} -q_{k,0}^*[\mathbf{H}(s_k)]^{\mathbf{H}}p_{k,0} & \cdots & -q_{k,0}^*[\mathbf{H}(s_k)]^{\mathbf{H}}p_{k,n_b} \\ \vdots & \ddots & \vdots \\ -q_{k,n_a}^*[\mathbf{H}(s_k)]^{\mathbf{H}}p_{k,0} & \cdots & -q_{k,0}^*[\mathbf{H}(s_k)]^{\mathbf{H}}p_{k,n_b} \end{bmatrix},$$

$$[\mathbf{W}_{22}] = \sum_{k \in I_k} |D(s_k)|^2 \begin{bmatrix} p_{k,0}^*[\mathbf{I}]p_{k,0} & \cdots & p_{k,0}^*[\mathbf{I}]p_{k,n_b} \\ \vdots & \ddots & \vdots \\ p_{k,n_b}^*[\mathbf{I}]p_{k,0} & \cdots & p_{k,n_b}^*[\mathbf{I}]p_{k,n_b} \end{bmatrix}, \tag{12}$$

where $[\mathbf{Q}(s)] = [\mathbf{H}(s)]^{\mathrm{H}}[\mathbf{H}(s)]$, $[\mathbf{I}]$ is the unity matrix, $p_{k,n} = q_{k,n} = s_k^n$ and the superscript $*$ represents complex conjugation.

The expression of elements along the principal diagonal of the error matrix is

$$J_{i,i}(\{\mathbf{\Theta}_i\}) = \{\mathbf{\Theta}_i\}^{\mathrm{T}}[\mathbf{W}]\{\mathbf{\Theta}_i\}, \quad i = 1, \ldots, N_i, \tag{13}$$

showing that the minimum value for every function $J_{i,i}$ corresponds to a null vector $\{\mathbf{\Theta}_i\}$. Therefore, in order to obtain a non-zero solution, a constraint must be introduced, namely,

$$\gamma(\{\mathbf{\Theta}_i\}) = \{\mathbf{\Theta}_i\}^{\mathrm{T}}[\mathbf{R}]\{\mathbf{\Theta}_i\} - 1 = 0, \tag{14}$$

where the value for matrix $[\mathbf{R}]$ is specified subsequently.

The minimization of function $J_{i,i}(\{\mathbf{\Theta}_i\})$ constrained by equation (14) can be performed by using Lagrange's multipliers [26], i.e., solving the system of equations

$$\partial J_{i,i}(\{\mathbf{\Theta}_i\})/\partial\{\mathbf{\Theta}_i\} - \lambda_i(\partial\gamma(\{\mathbf{\Theta}_i\})/\partial\{\mathbf{\Theta}_i\}) = 0, \qquad \gamma(\{\mathbf{\Theta}_i\}) = 0, \qquad i = 1, \ldots, N_i.$$

By considering equations (13) and (14) the first of these equations becomes

$$[\mathbf{W}]\{\mathbf{\Theta}_i\} - \lambda_i[\mathbf{R}]\{\mathbf{\Theta}_i\} = 0.$$

By multiplying the previous expression by $\{\mathbf{\Theta}_i\}^{\mathrm{T}}$ and using equation (14), it follows that

$$J_{i,i}(\{\mathbf{\Theta}_i\}) = \lambda_i,$$

so that the following relationship holds:

$$[\mathbf{W}]\{\mathbf{\Theta}_i\} - J_{i,i}(\{\mathbf{\Theta}_i\})[\mathbf{R}]\{\mathbf{\Theta}_i\} = 0, \qquad i = 1, \ldots, N_i. \tag{15}$$

The next step is to select a particular value for matrix [**R**]:

$$[\mathbf{R}] = \begin{bmatrix} [\mathbf{W}_{11}] & [\mathbf{0}] \\ [\mathbf{0}] & [\mathbf{0}] \end{bmatrix}.$$

By introducing matrix [**R**] into expression (15) the calculation can be simplified by recalling the structure of matrix [**W**] (11) and that of the coefficient matrix [**Θ**] (7):

$$[\mathbf{W}_{11}]\{\mathscr{A}_i\} + [\mathbf{W}_{12}]\{\mathscr{B}_i\} - J_{i,i}[\mathbf{W}_{11}]\{\mathscr{A}_i\} = \{\mathbf{0}\},$$

$$[\mathbf{W}_{12}]^{\mathrm{H}}\{\mathscr{A}_i\} + [\mathbf{W}_{22}]\{\mathscr{B}_i\} = \{\mathbf{0}\}, \quad i = 1, \ldots, N_i, \tag{16}$$

where $\{\mathscr{A}_i\}$ and $\{\mathscr{B}_i\}$ are the ith column of matrices $[\mathscr{A}]$ and $[\mathscr{B}]$ respectively. By multiplying the first of equations (16) with $[\mathbf{W}_{11}]^{-1}$ and taking advantage of the second, one obtains

$$([\mathbf{W}_{11}]^{-1}[\mathbf{W}_{12}][\mathbf{W}_{22}]^{-1}[\mathbf{W}_{12}]^{\mathrm{H}} - (1 - J_{i,i})[\mathbf{I}])\{\mathscr{A}_i\} = \{\mathbf{0}\}, \quad i = 1, \ldots, N_i, \tag{17}$$

By writing

$$1 - J_{i,i}(\{\mathbf{\Theta}_i\}) = \mu_i, \tag{18}$$

equation (17) becomes

$$([\mathbf{G}] - \mu_i[\mathbf{I}])\{\mathscr{A}_i\} = \{\mathbf{0}\}, \quad i = 1, \ldots, N_i \tag{19}$$

with

$$[\mathbf{G}] = [\mathbf{W}_{11}]^{-1}[\mathbf{W}_{12}][\mathbf{W}_{22}]^{-1}[\mathbf{W}_{12}]^{\mathrm{H}}. \tag{20}$$

A non-zero solution for equation (19) is obtained by evaluating the eigenvalues of the matrix [**G**]: according to equation (18) the maximum eigenvalue is that one for which the error $J_{i,i}(\{\mathbf{\Theta}_i\})$ is minimum. Moreover, since equation (19) is valid for every input i and matrix [**G**] does not depend on this input, this relation between errors and eigenvalues must be extended to all the N_i errors $J_{i,i}$, so that the first N_i eigenvalues and eigenvectors must be considered, the former being ranked in descending order. As a consequence, by solving only one eigenvalue problem, it is possible to estimate all the coefficients $\{\mathscr{A}_i\}$; coefficients $\{\mathscr{B}_i\}$ are evaluated in a following step through the second of equation (16).

To complete this frequency domain estimation algorithm it is necessary to assign the weighting function $D(s)$ introduced in equation (4). To perform this choice it is useful to recall that a weighting function is used in the smoothing technique by Dat and Meurzec [9] and in the global smoothing technique too [11]. In all these works every frequency response function was written as the ratio between two polynomials

$$H(s) = P(s)/Q(s),$$

and the weighting function was set as $D(s) = |Q(s)|^{-1}$, i.e., the inverse of the absolute value of the denominator (the rationale behind this choice is clearly explained in reference [11]).

According to equation (1) in this article it is assumed that

$$[\mathbf{H}(s)] = [\mathbf{B}(s)][\mathbf{A}(s)]^{-1},$$

so that the weighting function can be set as

$$D(s) = \| [\mathbf{A}(s)]^{-1} \|, \tag{21}$$

i.e., the norm of the inverse of the denominator polynomial matrix, similar to the original work by Dat and Meurzec.

Clearly, $D(s)$ can be set according to relation (21) only when a first estimate for the matrix $[\mathbf{A}(s)]$ is available. As a consequence, this procedure is iterative in nature; it is possible to start with $D(s) = 1$ and continue by introducing into $D(s)$ the last estimate of $\| [\mathbf{A}(s)]^{-1} \|$. This iterative procedure concludes when the error in the curve fitting, i.e., $J_{i,i}$, ceases to decrease.

4.3. NUMERICAL CONDITIONING

The estimation of coefficients in high order polynomials is often an ill-conditioned problem, mainly due to the structure of matrices involved in the numerical calculation. Clearly, ill-conditioning problems during the estimation of coefficients $[\mathbf{A}_r]$ and $[\mathbf{B}_r]$ lead to inaccurate estimates of the modal properties of the structure under investigation, requiring that this aspect must be addressed and fixed.

Different ways of solving numerical conditioning problems arising from the high order polynomials can be considered, as shown by Phillips and Allemang [25]. In the companion paper [11], Forsythe's orthogonal polynomials were selected [21], which were originally used for system identification in the orthogonal polynomial method proposed by Van der Auweraer and Leuridan in reference [22]. Anyway, it must be underlined that by assuming a common denominator model to apply the system identification procedure the application of orthogonal polynomial is rather simple. In contrast, when a matrix fraction description is used, implementing an orthogonal polynomial is a more complex task, requiring a particular algorithm to be established, as stated in reference [25] and demonstrated in the appendix of reference [22].

As a result, the other ways suggested by Phillips *et al.* have been analyzed, leading to the selection of scaling both the frequency axis and $[\mathbf{B}_r]$ coefficients. In particular, frequencies have been scaled according to

$$s' = \mathrm{j}\omega/(\omega_M/2), \tag{22}$$

where ω_M is the upper limit of the circular frequency range under analysis. Moreover, $[\mathbf{B}_r]$ coefficients have been scaled as

$$[\mathbf{B}_r'] = [\mathbf{B}_r]/H_M, \tag{23}$$

where H_M is the maximum modulus of measured FRFs in the considered frequency range. As stated in reference [25], this strategy led to great improvement in the conditioning number of the matrices to be inverted (in this procedure matrices $[\mathbf{W}_{11}]$ and $[\mathbf{W}_{22}]$).

4.4. EXTRACTION OF MODAL PARAMETERS

It is well known that the FRFs matrices relating output displacements to input forces can be written in terms of modal parameters as

$$[\mathbf{H}(s)] = \sum_{k=1}^{2N} \{\mathbf{V}_k\}(s-\lambda_k)^{-1} \lfloor \mathbf{L}_k \rfloor = [\mathbf{V}][s[\mathbf{I}] - [\mathbf{\Lambda}]]^{-1}[\mathbf{L}], \tag{24}$$

where [**V**] and [**L**] are mode shapes and modal participation factors matrices, respectively, [**Λ**] is the matrix with poles along the diagonal and the summation is extended to $2N$ (with N being the number of modes) to allow for poles appearing in complex conjugate pairs.

According to references [5] and [22], [$\mathbf{A}_r$] coefficients determined by using the procedure proposed in this article can be used to build the companion matrix, defined as

$$[\mathbf{A}_c] = \begin{bmatrix} [\mathbf{A}'_{n_a-1}] & [\mathbf{A}'_{n_a-2}] & \cdots & [\mathbf{A}'_1] & [\mathbf{A}'_0] \\ [\mathbf{I}] & [\mathbf{0}] & \cdots & [\mathbf{0}] & [\mathbf{0}] \\ [\mathbf{0}] & [\mathbf{I}] & \cdots & [\mathbf{0}] & [\mathbf{0}] \\ \vdots & \vdots & \ddots & \vdots & \vdots \\ [\mathbf{0}] & [\mathbf{0}] & \cdots & [\mathbf{I}] & [\mathbf{0}] \end{bmatrix}, \tag{25}$$

where

$$[\mathbf{A}'_r] = -[\mathbf{A}_{n_a}]^{-1}[\mathbf{A}_r], \quad r = 0, \ldots, n_a - 1.$$

The companion matrix is used to determine poles λ'_k and modal participation factors of the system under analysis by solving the eigenvalue problem

$$([\mathbf{A}_c] - \lambda'_k[\mathbf{I}])\{\mathbf{L}'_k\} = \{\mathbf{0}\}, \tag{26}$$

where $\{\mathbf{L}'_k\rangle$ is related to the kth modal participation factor according to

$$\{\mathbf{L}'_k\} = \begin{Bmatrix} \lambda_k'^{n_a-1}\{\mathbf{L}_k\} \\ \lambda_k'^{n_a-2}\{\mathbf{L}_k\} \\ \vdots \\ \{\mathbf{L}_k\} \end{Bmatrix}$$

and λ'_k are obtained according to the scaling scheme given by equation (22), so that the unscaled poles of the system are given by

$$\lambda_k = \lambda'_k \omega_M / 2. \tag{27}$$

Moreover, the kth modal participation factor can be extracted from the last N_i rows of the $\{\mathbf{L}'_k\}$ vector.

Finally, every pole λ_k is related to the corresponding natural circular frequency ω_k and damping ratio ζ_k by

$$\lambda_k = \omega_k(-\zeta_k + \mathrm{j}\sqrt{1 - \zeta_k^2}). \tag{28}$$

As a result, the natural circular frequency can be evaluated as

$$\omega_k = |\lambda_k|$$

and the damping ratio is given by

$$\zeta_k = -\,\mathrm{real}(\lambda_k)/\omega_k.$$

The matrix of mode shapes [**V**] can be estimated by using the global frequency domain least-squares procedure as shown in Appendix A.

5. APPLICATIONS

5.1. SIMULATED 5-DEGREES-OF-FREEDOM SYSTEM

The first application of the MIMO smoothing technique (MIMO-ST) is aimed at validating this new method by comparing its results, in terms of natural frequencies, damping ratios and synthesized FRFs (the latter being implicitly a validation of both modal participation factors and mode shapes), with those obtained by using another system identification technique. In particular, a MIMO method based on matrix rational polynomials and similar to the orthogonal polynomial technique [22] is used, where the numerical conditioning problem has been solved by applying the same procedure described in section 2.3 based on frequency and $[\mathbf{B}_r]$ coefficients scaling instead of using Forsythe's polynomials. For simplicity, this second technique is called MIMO improved rational polynomials (MIMO-IRP).

The system analyzed is shown in Figure 1: it has 5 degrees of freedom (d.o.f.) and the values for masses, rigidity of springs and damping of dash-pots have been chosen in order to obtain some modes with high damping ratios and the others with low damping ratios, so that it should be more difficult to identify correctly the latter with respect to the former.

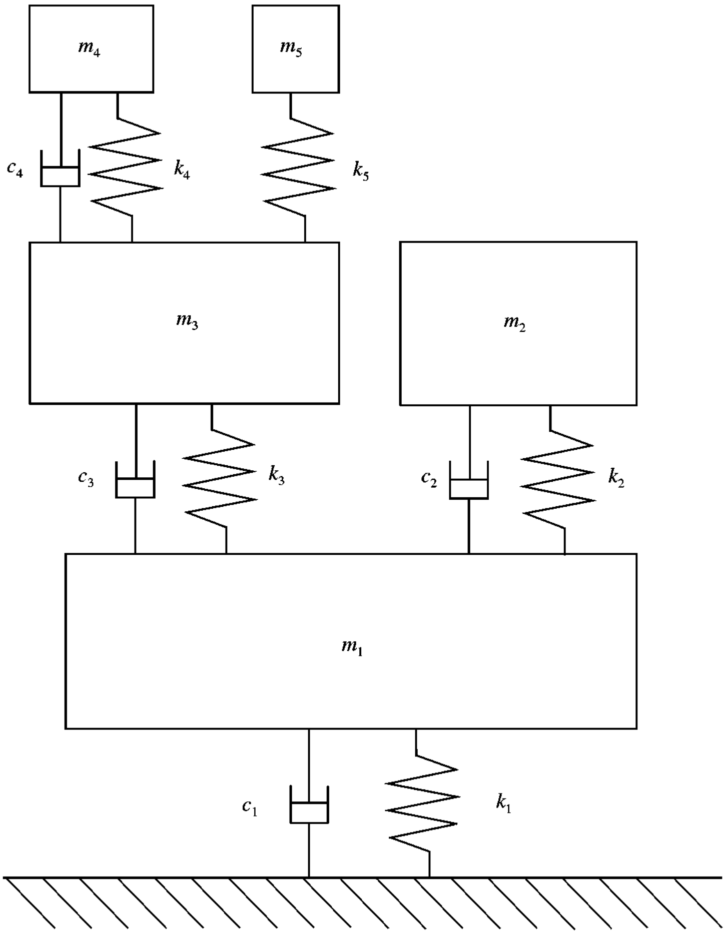

Figure 1. The 5-d.o.f. system analyzed.

TABLE 1

Comparison between results related to the 5-d.o.f. system

Correct values		MIMO-IRP		MIMO-ST	
f_n(Hz)	ζ_n(%)	f_n(Hz)	ζ_n(%)	f_n(Hz)	ζ_n(%)
7·1402	1·77	7·1425	1·76	7·1400	1·78
10·6721	4·31	10·6946	3·95	10·6747	4·40
13·5849	3·74	13·5967	3·49	13·5927	4·18
14·4868	0·82	14·4898	0·84	14·4875	0·86
17·3291	1·66	17·2890	1·59	17·3284	1·66

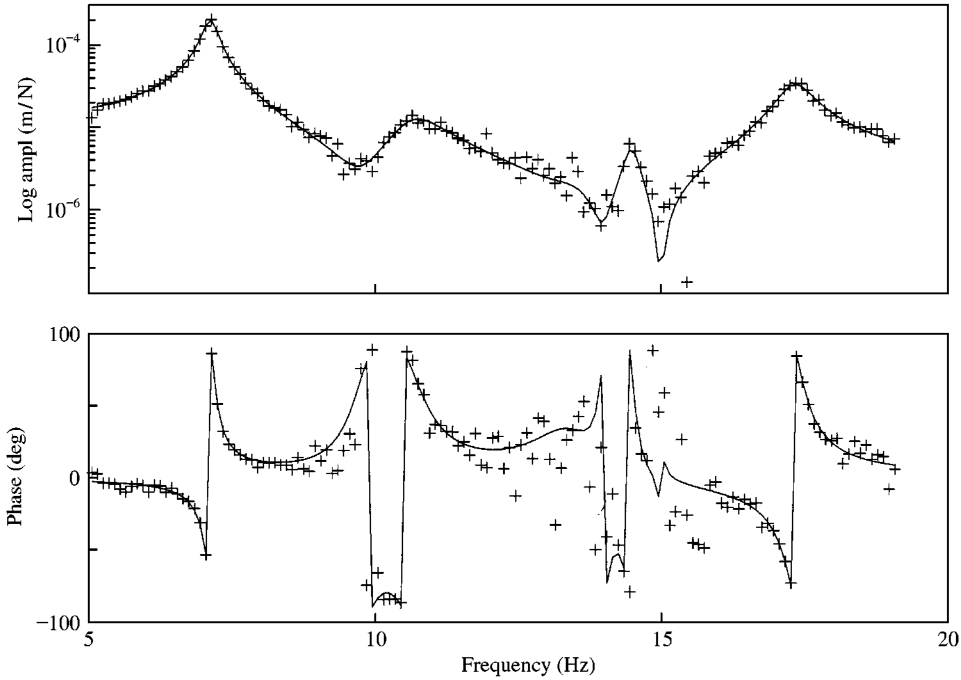

Figure 2. Results for the 5-d.o.f. system, FRF between both output and input at mass no. 3.

Analyzed frequency response functions have been calculated in the frequency range from 5 to 19 Hz by considering two inputs, one located at mass no. 3 and the other at mass no. 4, and displacements of all the five masses. Moreover, these data have been corrupted by both additive white noise (with standard deviation of 1×10^{-6}) and multiplicative white noise (2% of the maximum modulus of the considered FRFs).

Both the MIMO-ST and the MIMO-IRP have been applied on sub-intervals of the FRFs corrupted by disturbing noise. In both cases, the technique described in section 3 of reference [22] of increasing the order of the numerator to compensate for the effects of modes outside the frequency band under analysis by lower and upper residual terms has been applied.

Table 1 lists both correct values for natural frequencies and damping ratios of the system under analysis and corresponding results obtained by running the two considered techniques, showing that both provide very accurate estimations. Moreover, Figures 2 and 3 show the comparison between measured (crosses) and synthesized (continuous line)

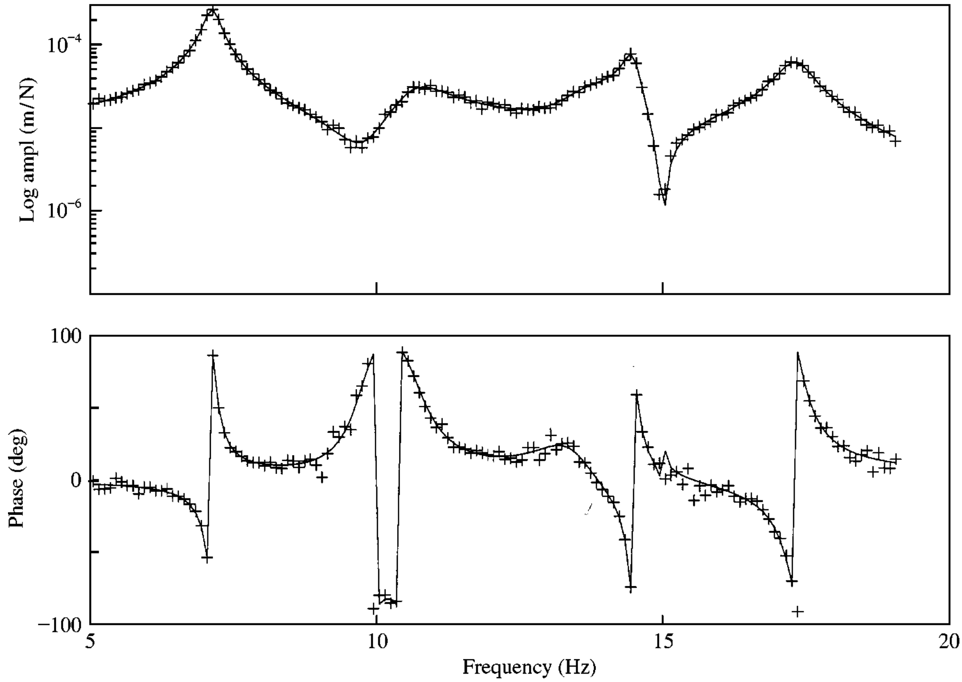

Figure 3. Results for the 5-d.o.f. system, FRF between output at mass no. 3 and input at mass no. 4.

FRFs, the latter being drawn by using results from either MIMO-ST or the other technique since corresponding curve fittings are almost superimposed.

5.2. AIRCRAFT FRF DATA

The aim of this second example is to demonstrate that the MIMO-ST is highly efficient in curve fitting FRF data measured from structural systems with high modal coupling and in the presence of disturbing noise.

In this example, data measured on an aircraft during the functionality check of the measurement and telemetry system performed on ground and before a flight-flutter test have been analyzed. Several locations on the aircraft structure were instrumented by placing accelerometers (more than 40), while the excitation was provided by the control surfaces that were activated through the flight control system (FCS) which generated a sweep sine function with starting and ending frequencies of 4 and 17 Hz respectively. Furthermore, due to the tight-flight testing schedule, it was impossible to adjust gains of the acquisition devices before every flight, with the result that often a discretization error occurred on measured signals. As a result, FRFs evaluated as the ratio between the output of the accelerometers and the signal generated by the FCS were characterized by a high level of noise in some frequency band. It follows that due to the modal coupling in the region between 11 and 14 Hz and to disturbing noise on the FRFs, it is difficult for classical techniques to yield accurate estimates for the modal properties of the aircraft.

The check was performed in two steps by injecting firstly a symmetric and secondly an antisymmetric input to the control surfaces, so that it is advisable to analyze the FRFs data

TABLE 2

Comparison between results related to the aircraft

MIMO-IRP		MIMO-ST	
f_n(Hz)	ζ_n(%)	f_n(Hz)	ζ_n(%)
5·94	2·12	5·95	1·27
7·91	1·09	7·94	1·10
9·61	2·46	9·42	1·28
10·63	2·94	10·64	1·84
11·03	2·99	11·06	2·18
11·92	2·42	11·73	1·69
12·85	0·79	12·43	1·16
13·31	1·18	13·37	3·29
13·54	1·47	13·37	1·47
14·61	1·53	14·70	1·48
16·15	3·29	16·13	3·87

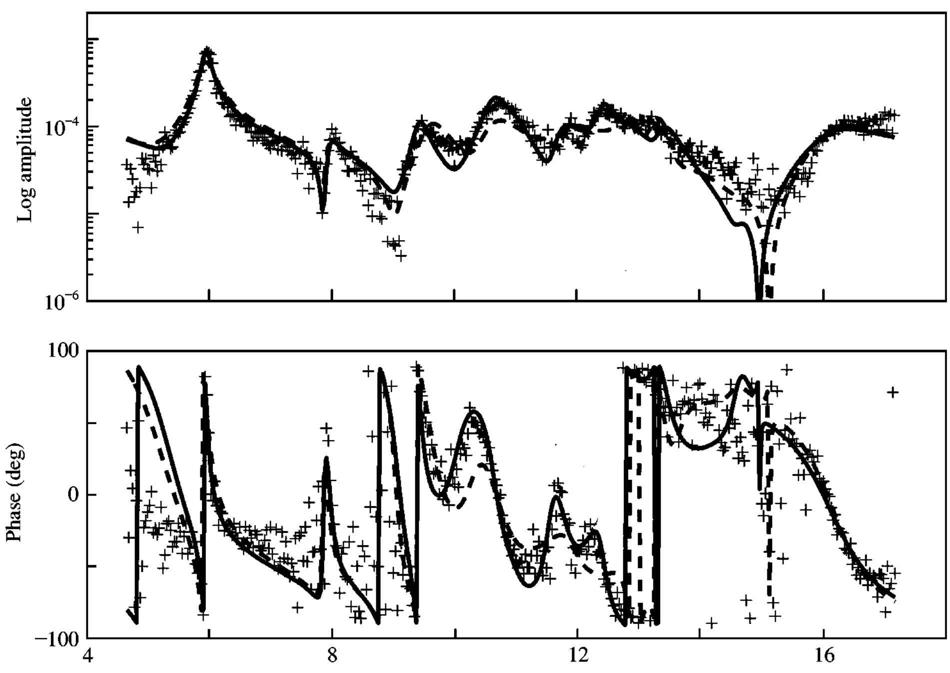

Figure 4. Results for aircraft FRFs, point 1, symmetrical input; ——, MIMO-ST; – – –, MIMO-IRP.

with a method that considers multiple input excitations, obtaining more accurate results in terms of modal properties of the aircraft.

Estimated natural frequencies and corresponding damping ratios obtained by using both the MIMO-ST and the MIMO-IRP, as in the previous example, are listed in Table 2. Both techniques has been run by dividing the entire frequency range into sub-intervals in order to simplify the analysis. In each sub-range, the MIMO-ST has been applied by starting with a given order of the polynomials at the denominator and increasing it (the order of the numerator is fixed accordingly and by taking into account out-of-band modes too). In the practical application of this technique it is of great importance to monitor the trend of the errors $J_{1,1}, \ldots, J_{N_i,N_i}$ since the best model is related to the lowest errors and a great increase in these errors is a symptom of an oversized order for the polynomials. Furthermore, it must be stressed that the procedure is not excessively time-consuming, provided that the calculation of matrices $[\mathbf{W}_{11}]$, $[\mathbf{W}_{12}]$ and $[\mathbf{W}_{22}]$ is performed by taking advantage of their particular structure. Conversely, the poles of the aircraft have been selected by using information provided by the stabilization diagram when the MIMO-IRP has been run.

It is clear that both methods provide similar results in terms of natural frequencies, even if only the MIMO-ST identifies the double pole at 13·37 Hz.

Figures 3–7 illustrate curve fitting obtained by both the MIMO-ST (continuous line) and the MIMO-IRP (dashed line) for two points located on the wing of the aircraft and for the two inputs (symmetric and antisymmetric). These figures clearly demonstrate that the MIMO-ST provides high-quality curve fitting, as well as the previous version proposed in reference [11], even if analyzed data are characterized by a low signal-to-noise ratio and there is a high modal coupling in the region between 11 and 14 Hz.

6. CONCLUSIONS

In a previous article [11] the global smoothing technique was presented and shown to be capable of determining the poles of structural systems for measured FRFs even when the

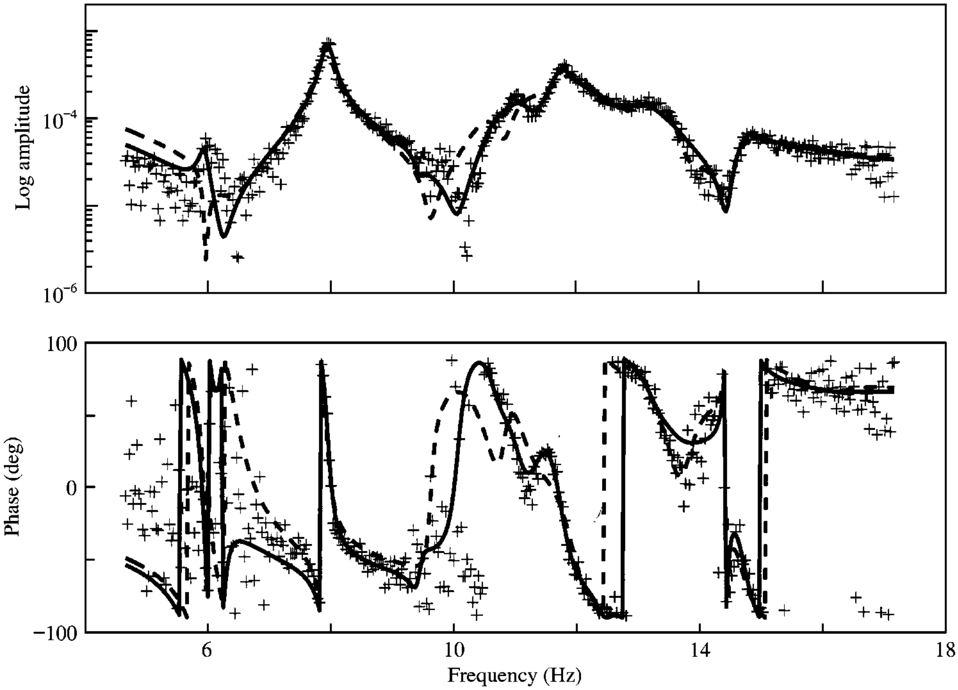

Figure 5. Results for aircraft FRFs, point 1, antisymmetrical input; ——, MIMO-ST; – – –, MIMO-IRP.

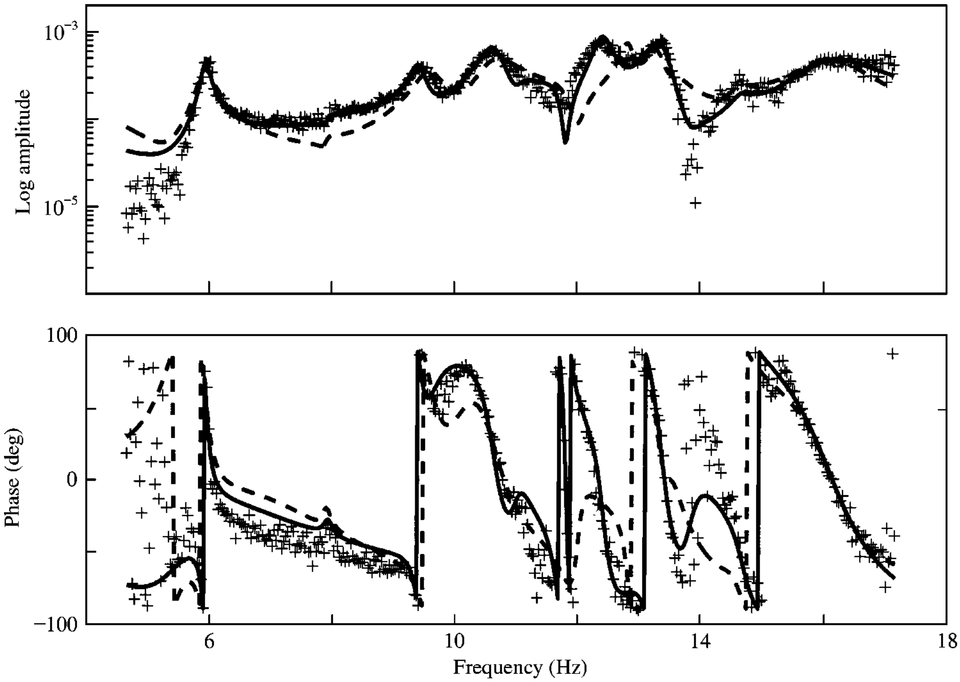

Figure 6. Results for aircraft FRFs, point 2, symmetrical input; ——, MIMO-ST; - - -, MIMO-IRP.

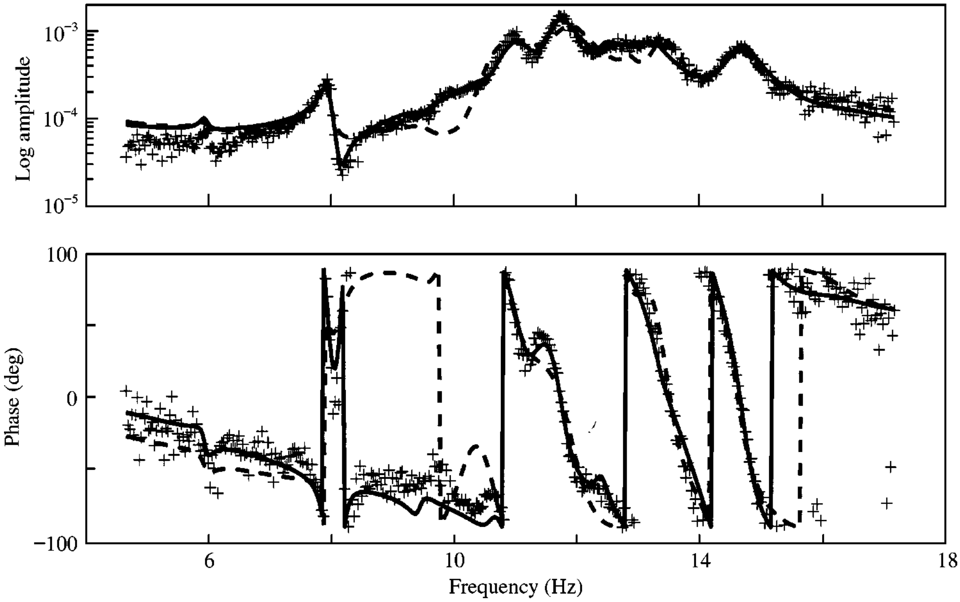

Figure 7. Results for aircraft FRFs, point 2, antisymmetrical input; ——, MIMO-ST; - - -, MIMO-IRP.

system exhibits complex dynamic behaviour due to high modal coupling. Nevertheless, that version of GST does not provide any estimate for the modal participation factors of the system under analysis, so that as many estimates for every mode shape will be obtained as the number of inputs to the considered system if a least-squares frequency domain method is applied.

In this article this difficulty has been overcome by proposing the extension of the global smoothing technique, properly developed in order to deal with systems with multiple-inputs and multiple-outputs.

This new method has been validated by presenting two different examples. The first demonstrated that this new version of the curve-fitting method provides accurate estimates for natural frequencies and damping ratios. The second, of interest in the aeronautical industry and related to FRFs measured on an aircraft before performing a flight-flutter test, clearly underlined the potential of the proposed method in terms of curve-fitting quality.

ACKNOWLEDGMENTS

The author would like to thank Dr D. M. Storer for very useful discussions about development and application of this method and the FIAT Research Center (CRF) for funding the research documented in this article.

REFERENCES

1. W. HEYLEN, S. LAMMENS and P. SAS 1995 *Katholieke Universiteit Leuven*. Modal analysis theory and testing.
2. H. VAN DER AUWERAER, W. LEURS, P. MAS and L. HERMANS 2000 *Proceedings* XVIII *International Modal Analysis Conference*. Modal parameter estimation from inconsistent data sets.
3. J. E. COOPER 1995 *Structures and Materials Panel Specialists' Meeting on "Advanced Aeroservoelastic Testing and Data Analysis", Rotterdam, AGARD-CP*-566. Parameter estimation methods for flight flutter testing.
4. N. M. M. MAIA and J. M. M. SILVA 1997 *Theoretical and experimental modal analysis*. Research Studies Press Ltd, New York: John Wiley & Sons Inc.
5. R. PINTELON, P. GUILLAUME and J. SCHOUKENS 1994 *IEEE Transactions on Automatic Control* **39**, 2245–2260. Parametric identification of transfer functions in the frequency domair—a survey.
6. S. O'F. FAHEY and J. PRATT 1998 *Experimental Techniques* **22**, 33–37. Frequency domain modal estimation techniques.
7. E. C. LEVI 1959 *IEEE Transactions Automatic Control* **AC-4**, 37–44. Complex-curve fitting.
8. C. K. SANATHANAN and J. KOERNER 1963 *IEEE Transactions Automatic Control* **AC-9**, 56–58. Transfer function synthesis as a ratio of two complex polynomials.
9. R. DAT and J. L. MEURZEC 1972 *La Recherche Aérospatiale* **4**, 209–215. Exploitation par Lissage Mathématique des Mesures d'Admittance d'un Systèm Linéaire.
10. F. FERRO 1990 *Degree thesis, Politecnico di Torino*. Optimization of a finite element model to correlate flight and ground vibration tests (in Italian).
11. R. RUOTOLO and D. M. STORER 2001 *Journal of Sound and Vibration* **239**, 41–56. A global smoothing technique for FRF data fitting.
12. D. R. GAUKROGER, C. W. SKINGLE and K. H. HERON 1973 *Journal of Sound and Vibration* **29**, 341–353. Numerical analysis of vector response loci.
13. H. G. D. GOYDER 1980 *Journal of Sound and Vibration* **68**, 209–230. Methods and application of structural modelling from measured frequency response data.
14. R. PINTELON, J. SCHOUKENS and P. GUILLAUME 1989 *Mechanical Systems and Signal Processing* **3**, 389–403. Parametric frequency domain modeling in modal analysis.
15. P. GUILLAUME, R. PINTELON and J. SCHOUKENS 1990 *Mechanical Systems and Signal Processing* **4**, 405–416. Description of a parametric maximum likelihood estimator in the frequency domain for multi-input, multi-output systems and its application to flight-flutter analysis.
16. H. VAN DER AUWERAER and P. GUILLAUME 1995 *Structures and Materials Panel Specialists' Meeting on "Advanced Aeroservoelastic Testing and Data Analysis", Rotterdam. AGARD-CP*-566. Maximum likelihood parameter estimation technique to analyse multiple input/multiple output flutter test data.
17. P. R. EMMETT, J. E. COOPER and J. R. WRIGHT 1995 *International Forum on Aeroelasticity and Structural Dynamics* 55.1–55.10. Improved frequency domain modal parameter identification.

18. J. E. COOPER, M. J. DESFORGES, P. R. EMMETT and J. R. WRIGHT 1995 *Structures and Materials Panel Specialists' Meeting on "Advanced Aeroservoelastic Testing and Data Analysis", Rotterdam, AGARD-CP*-566. Advances in the analysis of flight flutter test data.
19. R. RUOTOLO, W. BASSO and C. SURACE 1996 *Proceedings of Eurodyn '96*, 1125–1132. Flight flutter test data analysis.
20. R. RUOTOLO, D. M. STORER and L. TADDEUCCI 1997 *Proceedings* XV *International Modal Analysis Conference*. Development of a technique to determine the modal characteristics of structures using response data.
21. G. E. FORSYTHE 1957 *SIAM Journal* **5**, 74–88. Generation and use of orthogonal polynomials for data-fitting with a digital computer.
22. H VAN DER AUWERAER and J. LEURIDAN 1987 *Mechanical Systems and Signal Processing* **1**, 259–272. Multiple input orthogonal polynomial parameter estimation.
23. E. BALMÈS 1996 *Proceedings* XIV *International Modal Analysis Conference*, 540–546. Frequency domain identification of structural dynamics using the pole/residue parametrization.
24. E. A. MEDINA, R. D. IRWIN, J. R. MITCHELL and A. P. BUKLEY 1994 *The Journal of Astronautical Sciences* **42**, 113–129. MIMO system identification using frequency response data.
25. A. W. PHILLIPS and R. J. ALLEMANG 1996 *Proceedings 21st International Seminar on Modal Analysis, Leuven*, 1097–1109. Numerical considerations in modal parameter estimation.
26. J. W. DETTMAN 1969 *Mathematical Methods in Physics and Engineering*, New York: McGraw-Hill.

APPENDIX A

A global estimate for the modeshapes of the system under analysis can be obtained by using equation (24)

$$[\mathbf{H}(s)] = [\mathbf{V}][s[\mathbf{I}] - [\mathbf{\Lambda}]]^{-1}[\mathbf{L}] = [\mathbf{V}][\mathbf{P}(s)],$$

showing that the FRF matrix is given by the product of modeshapes, a constant matrix, and a function of both the s variable and of poles and modal participation factors of the system.

By evaluating the matrix $[\mathbf{P}(s)]$ at values s_k measured during the test using poles and modal participation factors estimated through the method proposed in this article, the previous equation leads to

$$[[\mathbf{H}(s_1)][\mathbf{H}(s_2)], \dots, [\mathbf{H}(s_m)]] = [\mathbf{V}][[\mathbf{P}(s_1)][\mathbf{P}(s_2)], \dots, [\mathbf{P}(s_m)]], \qquad (A1)$$

which can be rewritten as

$$[\mathbf{HH}] = [\mathbf{V}][\mathbf{PP}],$$

permitting estimation of the modeshape matrix by using the least-squares method.

Finally, as shown in reference [1], lower and upper residues can be easily introduced in equation (24) in order to accommodate modes outside the frequency range under analysis.